Multielectron contributions in elliptically polarized high-order harmonic emission from nitrogen molecules

Yuqing Xia and Agnieszka Jaroń-Becker*

JILA and Department of Physics, University of Colorado, Boulder, Colorado 80309-0440, USA
**Corresponding author: jaron@jila.colorado.edu*

Received November 21, 2013; revised January 25, 2014; accepted January 27, 2014;
posted January 29, 2014 (Doc. ID 201711); published March 7, 2014

We have studied the polarization and ellipticity of high-order harmonics from nitrogen molecules using the time-dependent density functional theory. The results of our numerical calculations are in excellent agreement with the data of recent experiments. The theoretical analysis of our results reveals that at least three contributions, namely those from the HOMO, the HOMO-1, and the HOMO-2 orbitals, contribute to the observed high harmonic spectra. Furthermore, we confirm that a proper account of the distribution of the alignment in the molecular ensemble is necessary to obtain agreement with the experimental data.

OCIS codes: (020.2649) Strong field laser physics; (270.4180) Multiphoton processes; (270.6620) Strong-field processes.
http://dx.doi.org/10.1364/OL.39.001461

High-order harmonic generation (HHG) is an important nonlinear process in the interaction between atoms and molecules and intense ultrashort laser pulses [1,2]. Presently, high harmonics are a tabletop light source of XUV and soft x-ray radiation [3] and single or trains of attosecond pulses [4–6], as well as zeptosecond waveforms [7]. According to the standard semiclassical three-step model of HHG [8], the generated signal strongly depends on the emission and recombination of an electron wavepacket with orbitals in an atom or molecule. Thus, properties of the emitted high harmonic radiation, such as amplitude, phase and polarization, depend on the properties of the target, e.g., the shape of the orbitals and the orientation of the molecule with respect to the laser polarization direction. Therefore, HHG is also an important spectroscopic tool to study the response of molecules to intense laser light [9–13].

Theoretically, HHG can be obtained as the Fourier transform of the dipole acceleration of the time-dependent multielectron wave function of the atom or molecule in the driving laser field. It is, however, challenging to compute the full laser-induced response of all electrons in a target. Thus, usually the single-active electron approximation is applied, in which the dynamics of one electron from a certain orbital is considered. Then, the harmonic power spectra of individual ionization and recombination channels are calculated and, if needed, they are summed up. Despite the fact that the limits of the single-active electron approximation are not fully explored, multielectron effects can be expected to be particularly important for molecules with closely lying orbitals in the neutral as well as the cation [14–16].

In this Letter, we present results of numerical calculations for the polarization and ellipticity of high-order harmonics from nitrogen molecules obtained using time-dependent density functional theory (TDDFT). Our results are in good agreement with the data of recent experiments [16,17] and reveal the importance of multielectron contributions from at least three different orbitals (HOMO, HOMO-1, and HOMO-2) in the molecule. In particular, we show that the contributions from inner-valence orbitals are significant at wavelengths at which there is a resonance between two orbitals. Furthermore, we confirm that it is essential to take proper account of the distribution of the internuclear axis with respect to the polarization direction in the molecular ensemble.

In order to consider multielectron effects in HHG in a molecule, we used TDDFT which has been proven to be very successful in determining optical properties of molecules and clusters. For noninteracting particles, TDDFT relies on a solution of the Kohn–Sham equations

$$i\frac{\partial}{\partial t}\phi_k(\mathbf{r},t) = -\nabla^2\phi_k(\mathbf{r},t) + (V_{\mathrm{KS}}[\rho(\mathbf{r},t)] + U(\mathbf{r},t))\phi(\mathbf{r},t), \tag{1}$$

where $\rho(\mathbf{r},t) = \sum_k \phi_k^*(\mathbf{r},t)\phi_k(\mathbf{r},t)$ is the density of the noninteracting particles, ϕ_k are the so-called Kohn–Sham orbitals, V_{KS} contains correlation and exchange interactions, which we have considered within the local density approximation in the present calculations, and $U(t)$ denotes the interaction of the Kohn–Sham orbitals with the external laser field. Since the Kohn–Sham orbitals are obtained for fictitious noninteracting particles and the interaction is considered via the external potential V_{KS}, there has been discussion about the interpretation of Kohn–Sham orbitals [18] and the relationship between Kohn–Sham eigenvalues and excitation energies have been studied [19,20].

The Kohn–Sham equations were solved for the interaction of the nitrogen molecule, initially in its ground state, with an intense laser pulse on a space–time grid with time step size of 0.05 a.u. and grid step size of 0.28 a.u. Detailed studies were performed to ensure convergence of the results. Using the Kohn–Sham orbitals at the end of the pulse we obtained the dipole moments $d_{\parallel}(\theta,t)$ and $d_{\perp}(\theta,t)$ parallel and perpendicular, respectively, to the polarization direction of the driving field for a given orientation θ of the molecular axis with respect to the polarization direction. To take account of

the distribution of alignment angles in a molecular ensemble in the experiment, it is customary [16,21] to average the dipole moments using the reported alignment distributions. Finally, we obtained the ellipticity of a given harmonic as [21,22]

$$\epsilon = \sqrt{\frac{1 + r^2 - \sqrt{1 + 2r^2\,\cos(2\delta) + r^4}}{1 + r^2 + \sqrt{1 + 2r^2\,\cos(2\delta) + r^4}}}, \qquad (2)$$

where $r = |d_\perp(\theta,\omega)|/|d_\parallel(\theta,\omega)|$ and $\delta = \arg[d_\perp(\theta,\omega]$–$\arg[d_\parallel(\theta,\omega]$.

Measurements of the polarization and ellipticity of high-order harmonics generated in nitrogen molecules have been reported recently [10,16]. Since ionization and high harmonic generation in molecules depend strongly on the angle between the molecular axis and the polarization direction, in the experiments a pump pulse was used to create a rotational wave packet in order to align the molecules along the polarization of the pump pulse every half-rotational period. The distribution of the alignment was estimated from the rotational temperature of the gas. By varying the relative angle between the probe pulse, which generates the harmonics, and the pump pulse, the polarization and ellipticity as a function of the molecular orientation in the ensemble was observed.

In Figs. 1 and 2, we present results of our calculations for the two recent experiments. In both figures, the ellipticity of the generated harmonics in the nitrogen molecule is shown as a function of harmonic order for different orientation of the molecular axis with respect to the polarization direction of the driving laser field. We

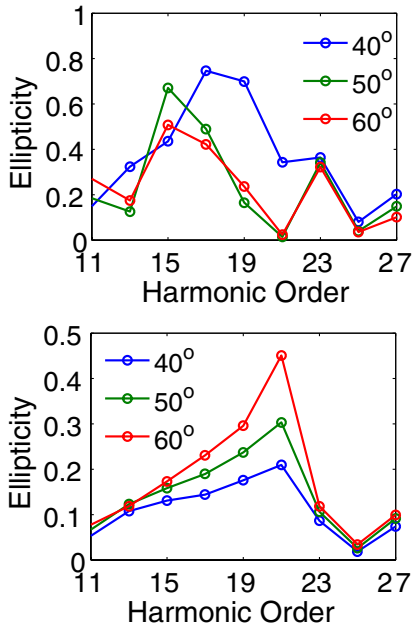

Fig. 1. Ellipticity of higher-order harmonics as a function of the harmonic orders for three molecular alignment angles at $\lambda = 800$ nm and peak intensity of $I_0 = 1 \times 10^{14}$ W/cm^2. Comparison of the results in which no average (upper panel) and a proper average (lower panel) over the distribution of the alignment in the molecular ensemble, as reported in the experiment [10], has been taken into account.

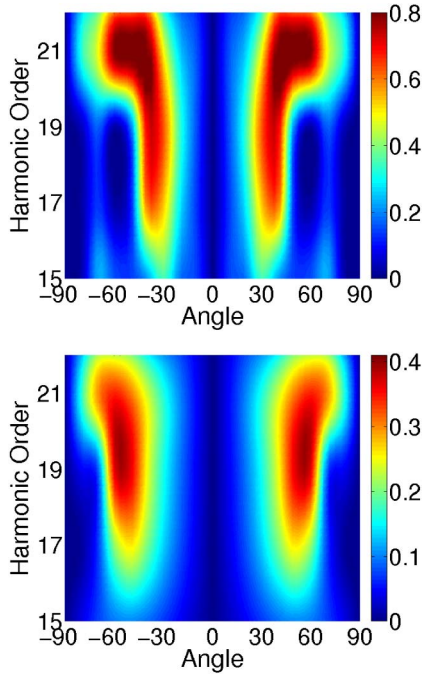

Fig. 2. Ellipticity of higher-order harmonics as a function of the molecular alignment angle and the order of the harmonics at $\lambda = 800$ nm and peak intensity $I_0 = 7.5 \times 10^{13}$ W/cm^2. Comparison of the results in which no average (upper panel) and a proper average (lower panel) over the distribution of the alignment in the molecular ensemble, as reported in the experiment [16], has been taken into account.

compare results obtained for a single fixed orientation of the molecular axis (upper panel) with the results of an ensemble average. In the latter, the results were averaged over the reported distribution of axis orientation in the ensemble (lower panel).

In agreement with both sets of experimental data [10,16], we obtain the largest variation of the ellipticity for harmonic orders above 17 up to the cutoff. For the ensemble average (lower panel), we find that the values are in quantitative agreement with the experimental observations showing in both cases a maximum ellipticity of about 0.3–0.5 for alignment angles around 40°–60°. We note that we found the best agreement with the experimental data for slightly lower peak intensities than reported. We attribute the sensitivity of the ellipticity as a function of intensity to the multielectron character within the present theoretical method. It has been shown by Son *et al.* [22], and confirmed by us in test calculations, that for one- and two-electron molecules the ellipticity varies more smoothly. The comparison with the results for a fixed orientation (upper panel) confirm the importance of the ensemble average over the distribution of the molecular alignment. In particular, the results in Fig. 1 (upper panel) show strong variations in the absolute value, the position of the maximum as well as the overall shape of the ellipticity as a function of harmonic order, which have not been observed in the experiment.

In previous theoretical analysis [16], harmonic generation from different HHG channels due to the dynamics in the ion was considered using the strong-field

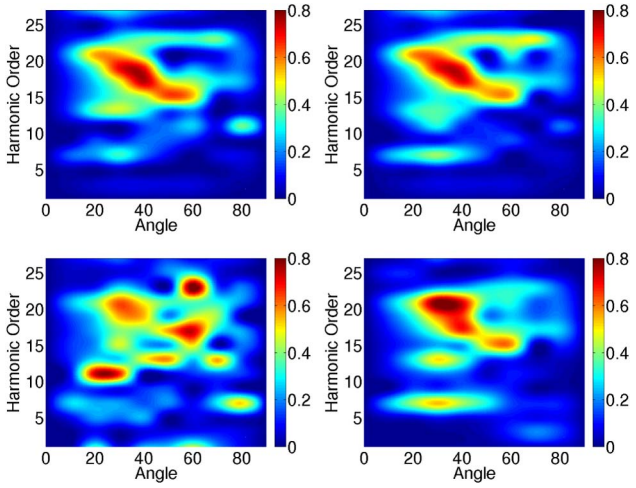

Fig. 3. Ellipticity of harmonics as function of harmonic order (vertical axis) and angle between molecular axis and laser polarization direction (horizontal axis). Comparison of results from the full calculation (upper left panel) and contributions from HOMO, HOMO-1, and HOMO-2 (upper right panel), HOMO and HOMO-1 (lower right panel), and HOMO only (lower left panel). Laser parameters: wavelength of 800 nm, peak intensity of 1×10^{14} W/cm^2, and pulse duration of 20 fs.

eikonal-Volkov approximation incorporating laser field-free ionic scattering states. In particular, three ionic states, namely the ground $X^2\Sigma_g$ and the excited $A^2\Pi_u$ and $B^2\Sigma_u$ states, have been included to account for the dynamics in the molecular ion between ionization and recombination. For each HHG channel, the single-active electron approximation was used but interferences between the channels and subcycle excitation dynamics in the cation between ionization and recombination of the electron were considered as well. It has been pointed out that for orientation angles larger than 50°, mainly the $X^2\Sigma_g$ and $A^2\Pi_u$ states, contribute to the observed large ellipticity of the harmonics, while channels associated with the $B^2\Sigma_u$ state are less important.

In our full TDDFT calculations, the response of all electrons in the nitrogen molecule is considered. Due to the *ab initio* character of TDDFT calculations and in contrast to other theoretical approaches, e.g., the strong-field approximation used in [16], the recombination and ionization events cannot be separated in the analysis and the laser driven dynamics is not restricted to part of the pulse. In order to analyze the role of transitions to individual orbitals, we have further calculated the responses from a subset of occupied orbitals in the molecule. In Fig. 3, we compare the results of such calculations with those of the full calculations for the same laser parameters as in Fig. 1. In each panel, the ellipticity of the harmonics is plotted as function of the harmonic order and the molecular alignment angle. In order to illustrate the importance of the inner-valence orbitals, no ensemble average of the molecular alignment was performed in this set of calculations.

The role of inner-shell contributions becomes obvious from the comparison of the results of the full calculation (upper left panel) and those obtained from the HOMO orbital only (lower left panel). Neither for the low-order nor for the high-order harmonics did the HOMO contribution agree well with the full results. A significant improvement is achieved when both contributions from the HOMO and the HOMO-1 orbitals are included in the calculations (lower right panel). However, certain features in the results of this partial calculation, such as the strong maximum for the 21st harmonic at an orientation angle of about 30°, are not present in the full calculation. Further inclusion of the contributions from the HOMO-2 orbital (upper right panel) finally leads to a more satisfactory agreement with the full results. Therefore, we may point out that we observe a strong influence of multielectron effects and contributions from at least three orbitals in the nitrogen molecule over the whole HHG spectrum. This applies, in particular, also for the low-order harmonics which could not be investigated in the previous theoretical studies based on strong-field approximation.

Thus, our multielectron calculations show within TDDFT calculations the relevance of at least three contributions directly related to HOMO, HOMO-1, and HOMO-2 orbitals and their coupling for the HHG process in nitrogen molecules. In our calculations, we have further noticed that a certain inner-shell channel becomes particularly important at driving laser wavelengths for which there is a resonance transition between the inner-shell orbital and the HOMO. This can be seen from the results presented in Fig. 4 which were obtained for a laser wavelength of 1000 nm. At this wavelength, the (unperturbed) HOMO and HOMO-2 levels in the neutral nitrogen molecule are coupled via a two-photon resonance transition. The results show that the effect of the HOMO-2 contributions on the ellipticity of the harmonics is even stronger than at 800 nm (Fig. 3).

In conclusion, results obtained within the time-dependent density functional theory show the importance of multielectron contributions for the interpretation of recent experimental data for the ellipticity of higher-order harmonics from nitrogen molecules. It is shown that the full multielectron results, which are in excellent agreement with the experimental data, contain essential contributions from the HOMO, the HOMO-1, and the HOMO-2 orbitals over the whole HHG spectrum. Furthermore, we have confirmed that it is essential to take proper

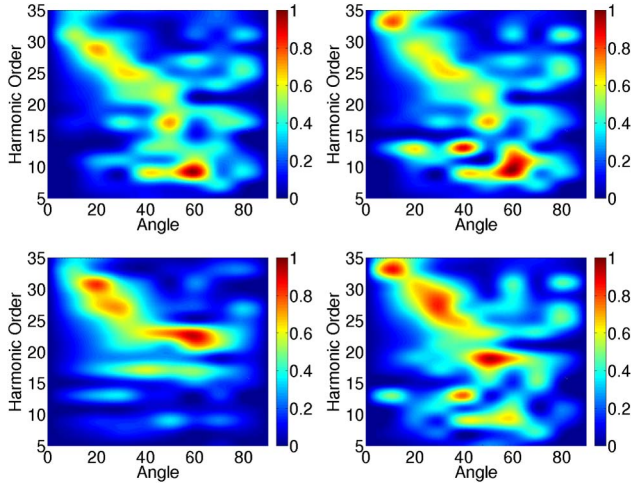

Fig. 4. Same as Fig. 3 but for a laser wavelength of 1000 nm.

account of the distribution of the molecular axis with respect to the polarization direction to find agreement with the observations.

This work was supported by the U.S. National Science Foundation (Grant No. PHY-1068706). A. J.-B. further acknowledges financial support by the U.S. National Science Foundation (Grant No. PHY-1125844). This work utilized the Janus supercomputer, which is supported by the National Science Foundation (Award No. CNS-0821794) and the University of Colorado Boulder. The Janus supercomputer is a joint effort of the University of Colorado Boulder, the University of Colorado Denver, and the National Center for Atmospheric Research.

References

1. A. McPherson, G. Gibson, H. Jara, T. S. Luk, I. A. McIntyre, K. Boyer, and C. K. Rhodes, J. Opt. Soc. Am. B **4**, 595 (1987).
2. M. Ferray, A. L'Huillier, X. F. Li, L. A. Lompre, G. Mainfray, and C. Manus, J. Phys. B **21**, L31 (1988).
3. T. Popmintchev, M.-C. Chen, D. Popmintchev, P. Arpin, S. Brown, S. Alisauskas, G. Andriukaitis, T. Balciunas, O. D. Mücke, A. Pugzlys, A. Baltuska, B. Shim, S. E. Schrauth, A. Gaeta, C. Hernandez-Garcia, L. Plaja, A. Becker, A. Jaron-Becker, M. M. Murnane, and H. C. Kapteyn, Science **336**, 1287 (2012).
4. I. P. Christov, M. M. Murnane, and H. C. Kapteyn, Phys. Rev. Lett. **78**, 1251 (1997).
5. M. Hentschel, R. Kienberger, C. Spielmann, G. A. Reider, N. Milosevic, T. Brabec, P. Corkum, U. Heinzmann, M. Drescher, and F. Krausz, Nature **414**, 509 (2001).
6. P. M. Paul, E. S. Toma, P. Breger, G. Mullot, F. Augé, Ph. Balcou, H. G. Muller, and P. Agostini, Science **292**, 1689 (2001).
7. C. Hernandez-Garcia, J. A. Perez-Hernandez, T. Popmintchev, M. M. Murnane, H. C. Kapteyn, A. Jaron-Becker, A. Becker, and L. Plaja, Phys. Rev. Lett. **111**, 033002 (2013).
8. P. B. Corkum, Phys. Rev. Lett. **71**, 1994 (1993).
9. M. Lein, J. Phys. B **40**, R135 (2007).
10. X. B. Zhou, R. Lock, W. Li, N. Wagner, M. M. Murnane, and H. C. Kapteyn, Phys. Rev. Lett. **100**, 073902 (2008).
11. W. Boutu, S. Haessler, H. Merdji, P. Breger, G. Waters, M. Stankiewicz, L. J. Frasinski, R. Taieb, J. Caillat, A. Maquet, P. Monchicourt, B. Carre, and P. Salieres, Nat. Phys. **4**, 545 (2008).
12. H. J. Wörner, J. B. Bertrand, D. V. Kartashov, P. B. Corkum, and D. M. Villeneuve, Nature **466**, 604 (2010).
13. C. Vozzi, C. Negro, F. Calegari, G. Sansone, M. Nisoli, S. DeSilvestri, and S. Stagira, Nat. Phys. **7**, 822 (2011).
14. W. Li, X. Zhou, R. Lock, S. Patchkovskii, A. Stolow, H. C. Kapteyn, and M. M. Murnane, Science **322**, 12070 (2008).
15. O. Smirnova, Y. Mairesse, S. Patchkovskii, N. Dudovich, D. Villeneuve, P. Corkum, and M. Yu. Ivanov, Nature **460**, 972 (2009).
16. Y. Mairesse, J. Higuet, N. Dudovich, D. Shafir, B. Fabre, E. Mevel, E. Constant, S. Patchkovskii, Z. Walters, M. Yu. Ivanov, and O. Smirnova, Phys. Rev. Lett. **104**, 213601 (2010).
17. X. Zhou, R. Lock, N. Wagner, W. Li, H. C. Kapteyn, and M. M. Murnane, Phys. Rev. Lett. **102**, 073902 (2009).
18. R. Stowasser and R. Hoffmann, J. Am. Chem. Soc. **121**, 3414 (1999).
19. A. Savin, C. J. Umrigar, and X. Gonze, Chem. Phys. Lett. **288**, 391 (1998).
20. E. J. Baerends, O. V. Gritsenko, and R. Van Meer, Phys. Chem. Chem. Phys. **15**, 16408 (2013).
21. A.-T. Le, R. R. Lucchese, and C. D. Lin, Phys. Rev. A **82**, 023814 (2010).
22. S.-K. Son, D. A. Telnow, and S. I. Chu, Phys. Rev. A **82**, 043829 (2010).